

A comparative study of energy transfer in dye mixtures in monomer and polymer matrices under pulsed laser excitation

M. Kailasnath^{a,*}, P.R. John^b, P. Radhakrishnan^a, V.P.N. Nampoori^a, C.P.G. Vallabhan^c

^a International School of Photonics, Cochin University of Science and Technology, Kochi 682022, India

^b Department of Applied Chemistry, Cochin University of Science and Technology, Kochi 682022, India

^c Centre of Excellence in Lasers and Optoelectronic Sciences, Cochin University of Science and Technology, Kochi 682022, India

Received 15 June 2007; received in revised form 23 August 2007; accepted 25 September 2007

Available online 29 September 2007

Abstract

This study was conducted to identify the concentration dependence of the operating wavelengths and the relative intensities in which a dye mixture doped polymer optical fibre can operate. A comparative study of the radiative and Forster type energy transfer processes in Coumarin 540:Rhodamine 6G, Coumarin 540:Rhodamine B and Rhodamine 6G:Rhodamine B in methyl methacrylate (MMA) and poly(methyl methacrylate) (PMMA) was done by fabricating a series of dye mixture doped polymer rods which have two emission peaks with varying relative intensities. These rods can be used as preforms for the fabrication of polymer optical fibre amplifiers operating in the multi-wavelength regime. The 445 nm line from an Nd:YAG pumped optical parametric oscillator (OPO) was used as the excitation source for the first two dye pairs and a frequency doubled Nd:YAG laser emitting at 532 nm was used to excite the Rh 6G:Rh B pair. The fluorescence lifetimes of the donor molecule in pure form as well as in the mixtures were experimentally measured in both monomer and polymer matrices by time-correlated single photon counting technique. The energy transfer rate constants and transfer efficiencies were calculated and their dependence on the acceptor concentration was analysed. It was found that radiative energy transfer mechanisms are more efficient in all the three dye pairs in liquid and solid matrices.

© 2007 Elsevier B.V. All rights reserved.

Keywords: Optical fibre preform; Energy transfer; Methyl methacrylate; Transfer efficiency; Fluorescence

1. Introduction

Several techniques have been reported for obtaining two or more wavelengths simultaneously from a single dye laser [1–4]. These techniques have used a number of wavelength selective elements in the dye laser cavity. The excitation of dye lasers through energy transfer processes by using an appropriate mixture of dyes is a more convenient means of extending the lasing wavelength region and improving the efficiency. Energy transfer dye lasers (ETDLs) using numerous donor–acceptor pairs have been reported by various workers during last three decades [5–10]. The primary motivation for the use of mixture of dyes as lasing medium has been either an improvement in the laser performance or the possibility of multi-wavelength operation. Dienes and Madden [11] developed a simple theoretical model to explain the variation of laser gain with acceptor concentration

and gain measurements done by them on Rhodamine 6G:resyl violet (Rh 6G–CV) mixtures and on CV alone clearly show a higher gain in the mixture as compared to CV alone [12]. This gain, which is the result of an enhanced lifetime of the acceptor, produces a blue shift in the emission peak of the acceptor [13]. As a result of this gain enhancement the conversion efficiency of the dye laser was improved considerably.

Most of the ETDL studies conducted earlier report investigations of energy transfer between dyes in liquid media. The use of a solid matrix for the dye laser gets rid of many of the common problems associated with static or flowing liquid systems such as convective Schlieren, evaporation, flow fluctuation, stagnant films, solvent or dye poisoning and even explosions [14]. One of the important advantages of transparent polymers compared to the traditional optical materials is that it is possible to introduce organic dyes or other compounds that can play the role of active components into the polymers, which appreciably changes the characteristics of the polymer matrix.

Vast majority of optical amplifiers are based on an optic fibre doped with a fraction of a percent of the rare-earth element

* Corresponding author. Tel.: +91 4842575848; fax: +91 4842576714.
E-mail address: kailas@cusat.ac.in (M. Kailasnath).

erbium. Although rare-earth doping has been generally used in silica, many laboratories have been working to develop stable rare-earth doped polymer lasers and amplifiers. The main issue with rare-earth doped polymer lasers and amplifiers has been pumping inefficiencies due to the de-excitation of the excited states caused by the IR absorption in the polymer. In bulk form, polymer hosts impregnated with certain dyes have achieved 80% conversion efficiency from pump power to signal power with tuning range close to those in solution [15]. Dye-doped polymer optical fibres can be made into useful fibre amplifiers and lasers that operate at wavelengths other than 1300 and 1550 nm [16,17]. Optical amplifiers and lasers made of dye-doped fibre require much less pump power compared to bulk material because of the effective confinement and long interaction length available in the fibre. Since photo bleaching increases with the increase of the exposure intensity, low pump intensity would increase the lifetime of the gain medium. Also, the thin and long geometry of the fibre is ideal for good thermal relaxation to minimize the thermally induced photo bleaching [18]. In this paper, we make a comparative study of energy transfer mechanisms in three different dye mixtures in monomer and polymer matrices under pulsed laser excitation.

2. Theoretical tools

The rate constants for the radiative and Forster type energy transfer mechanisms can be obtained from the Stern–Volmer plots given by the equations [19,20]:

$$\frac{I_{0d}}{I_d} = 1 + K\tau_{0d}[A] \quad (1)$$

$$\frac{\phi_{0d}}{\phi_d} = 1 + K_{nr}\tau_{0d}[A] \quad (2)$$

where I_{0d} and I_d are the fluorescence intensities of the donor in the absence and presence of acceptor, respectively; ϕ_{0d} and ϕ_d the corresponding quantum yields; τ_{0d} the fluorescence lifetime of the donor without acceptor; K and K_{nr} the total and non-radiative transfer rate constants, respectively and $[A]$ is the acceptor concentration. By knowing the value of τ_{0d} , K and K_{nr} can be calculated from the slopes of I_{0d}/I_d versus $[A]$ curve and ϕ_{0d}/ϕ_d versus $[A]$ curve which are straight lines. The critical transfer radius (R_0), for which energy transfer from the excited donor (D^*) to $[A]$ and emission from D^* are equally probable, is given by [21]

$$R_0 = \frac{7.35}{([A]_{1/2})^{1/3}} \quad (3)$$

where $[A]_{1/2}$ is the half quenching concentration which can be obtained under the condition:

$$\frac{I_{0d}}{I_d} = 2$$

Total transfer efficiency η is written as the sum of two parts:

$$\eta = \eta_r + \eta_{nr} \quad (4)$$

As is well known, in the presence of acceptor, the fluorescence intensity of the donor is reduced from I_{0d} to I_d by energy transfer to acceptor. A more practical expression for η can be given by [22,23]

$$\eta = 1 - \frac{I_d}{I_{0d}} \quad (5)$$

The non-radiative transfer efficiency η_{nr} is defined as [24]

$$\eta_{nr} = \pi^{1/2} X \exp(X^2)(1 - \operatorname{erf} X) \quad (6)$$

where $X = [A]/[A_0]$ is the molar concentration expressed relative to the critical molar concentration of the acceptor:

$$[A]_0 = \frac{3000}{2\pi^{3/2}NR_0^3}$$

where N is the Avogadro number and

$$\operatorname{erf} X = \frac{2}{\pi^{1/2}} \int_0^X \exp(-t^2) dt$$

3. Experimental

Three types of dye mixtures in MMA with fixed donor concentrations were prepared using laser grade dyes (Exciton, Lambda Physik) and distilled spectroscopic grade methyl methacrylate (Lancaster). The excitation source was a 10 ns pulsed Nd:YAG laser pumped Optical Parametric Oscillator (Spectra Physics-MOPO 710) tuned to 445 nm. This beam is employed to pump C 540 which is the donor molecule in the first two dye pairs whereas the Rh 6G:Rh B dye mixture was pumped using a frequency doubled Nd:YAG laser emitting at 532 nm. The pump wavelength 445 nm was selected since any higher pump wavelength, was found to be absorbed significantly by the Rh B and Rh 6G which results in the direct excitation of the acceptors. For the first two pairs, the donor concentration $[D]$ was kept fixed at 10^{-5} m/l and for the third pair, $[D]$ was fixed at 10^{-4} m/l while the acceptor concentration was varied.

Dye solution was taken in a quartz cuvette of width 1 cm and it was pumped in a transverse pumping configuration. The fluorescence emission from the solution was collected using an optical fibre and was directed to the entrance slit of an Acton Spectrapro-500i spectrograph having a resolution of 0.03 nm coupled with a CCD camera to record the spectrum. Optical absorption spectra of the samples were recorded on a Jasco V-570 spectrophotometer. The solutions were thermally polymerised after adding polymerisation initiator benzoyl peroxide (BPO) 0.4 wt.% and the chain transfer agent (*n*-butyl mercaptan), 0.1 wt.%. One end face of the fabricated rods was cut and polished and it was tightly fixed inside a hole drilled in an aluminium block, which is provided with openings for excitation of the sample and collection of fluorescence. All the samples had diameter of 1.2 cm and a length around 10 cm. No correction for the fluorescence reabsorption has been made as all the samples were of low concentration ($<10^{-3}$ m/l). The fluores-

cence lifetimes of the donor in pure form and in the dye mixture were measured both in MMA as well as PMMA matrices using time-correlated single photon counting technique employing a micro channel plate photomultiplier tube (Hamamatsu R 3809 U-50) and a multi-channel analyser. The measurement is made using an IBH-5000 Single Photon Counting Spectrometer. Two nano-LEDs (Spectra Physics) emitting at 455 and 495 nm with a resolution of 200 ps were used as the excitation sources. The fluorescence decay curves are analysed using an iterative fitting program provided by IBH and no further deconvolution was made.

4. Results and discussion

The fabricated sets of rods used in the present study are shown in Fig. 1 (a, C 540:Rh B; b, C 540:Rh 6G; c, Rh 6G:Rh B). Relevant absorption spectra of C 540, Rh B and Rh 6G as well as the emission spectra of C 540 and Rh 6G in PMMA matrix are presented in Fig. 2. Since most of the area under the emission line shapes of C 540 overlaps with the absorption line shapes of Rh 6G and Rh B, energy transfer from C 540 to Rh 6G and Rh B are clearly possible and the extent of this depends on the overlapping area. A similar kind of overlap exists between Rh 6G emission and Rh B absorption also.

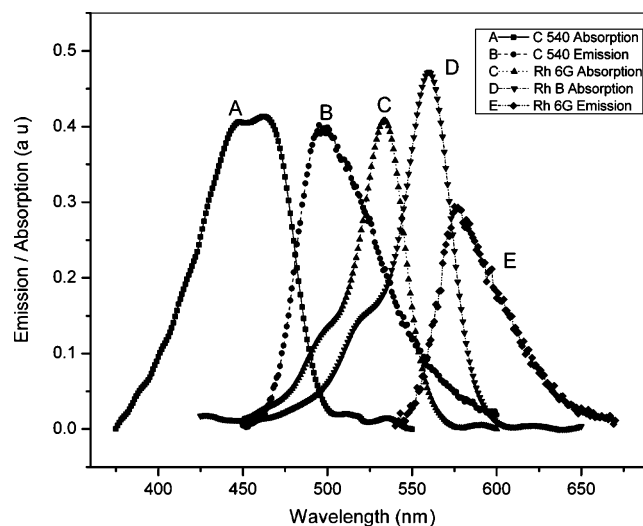


Fig. 2. Emission spectra of C 540 and Rh 6G along with absorption spectra of C 540, Rh 6G and Rh B in PMMA.

Figs. 3 and 4 represent the fluorescence spectra of the three dye pairs, in MMA as well as in PMMA matrices, respectively. It can be seen that the intensities and peak wavelengths are different in both matrices. These changes can be attributed to the

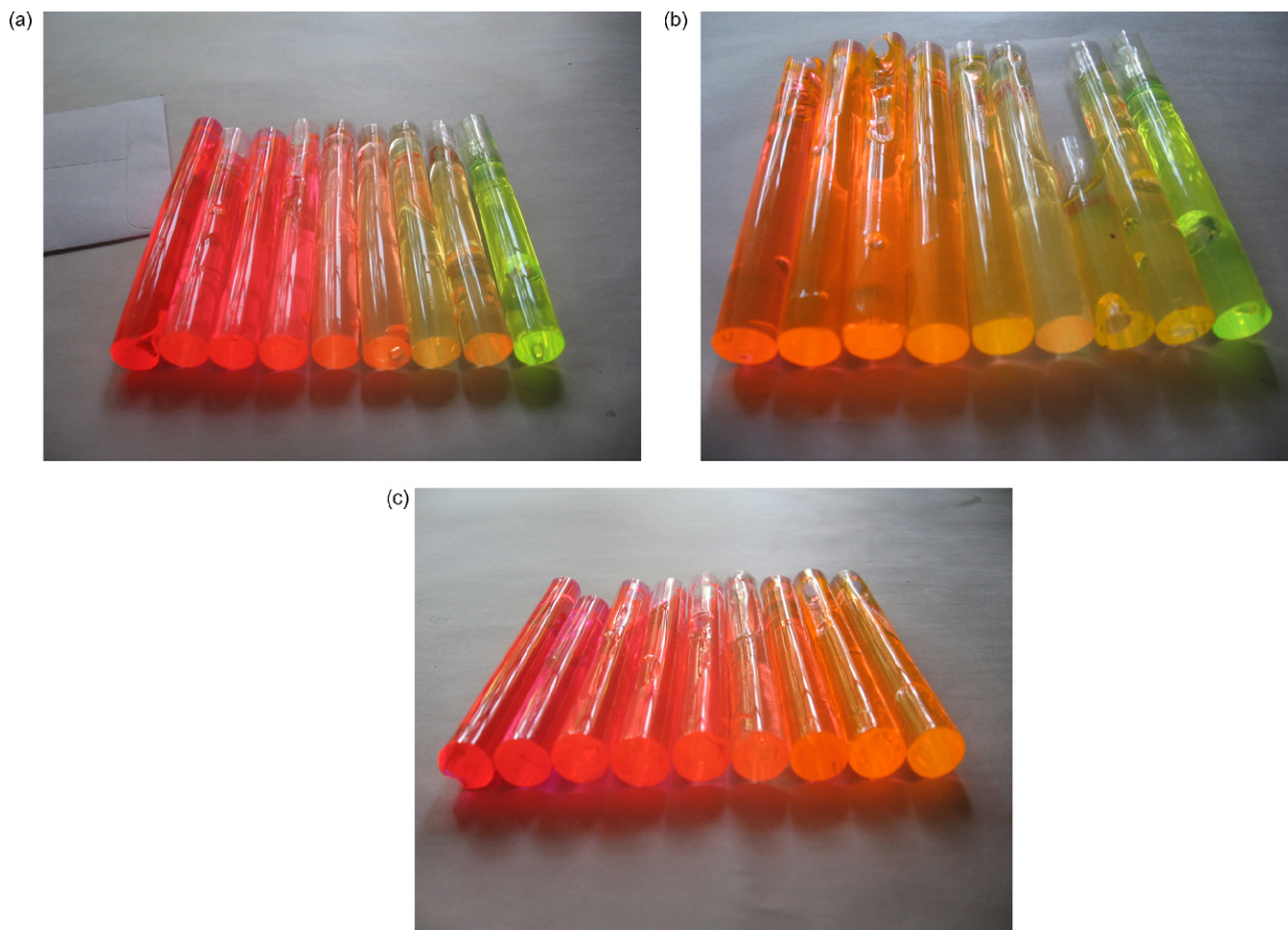


Fig. 1. (a)–(c) Photographs of all the three sets of fabricated dye mixture doped polymer rods.

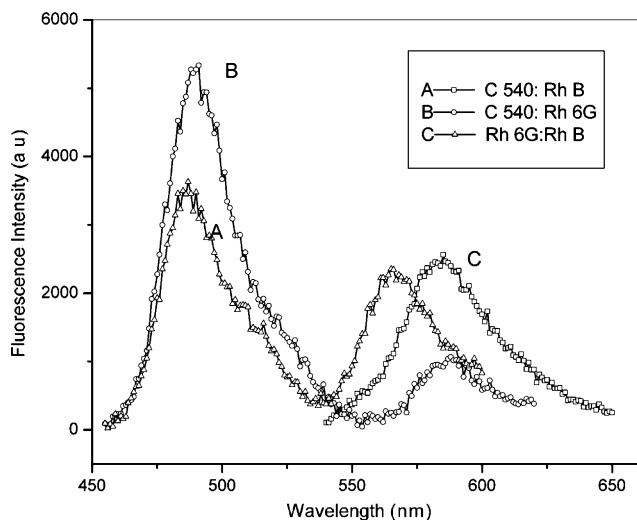


Fig. 3. Emission spectra of the dye mixtures in MMA. (A) $[D] = 10^{-5} \text{ mol l}^{-1}$ and $[A] = 7 \times 10^{-5} \text{ mol l}^{-1}$, (B) $[D] = 10^{-5} \text{ mol l}^{-1}$ and $[A] = 5 \times 10^{-4} \text{ m/l}$, (C) $[D] = 10^{-4} \text{ m/l}$ and $[A] = 5 \times 10^{-5} \text{ m/l}$.

volume reduction that is happening during the polymerisation of the MMA.

Detailed analysis of the evolution of the peak wavelengths and intensities is possible from Figs. 5 and 6, which are the spectra, recorded in MMA and PMMA, respectively, for different acceptor concentrations in the pair C 540:Rh 6G with a fixed donor concentration of 10^{-5} m/l . It is evident that there is considerable decrease in the fluorescence intensity after solidification. Due to the volume reduction, it was also observed that half quenching concentrations of all the three dye pairs have changed appreciably to a lower value. This is attributed to the fact that due to the effect of volume reduction, the donor and acceptor molecules are brought more close together, which enhances the quenching.

It was also observed that the acceptor concentration at which the two wavelengths producing comparable intensities are also

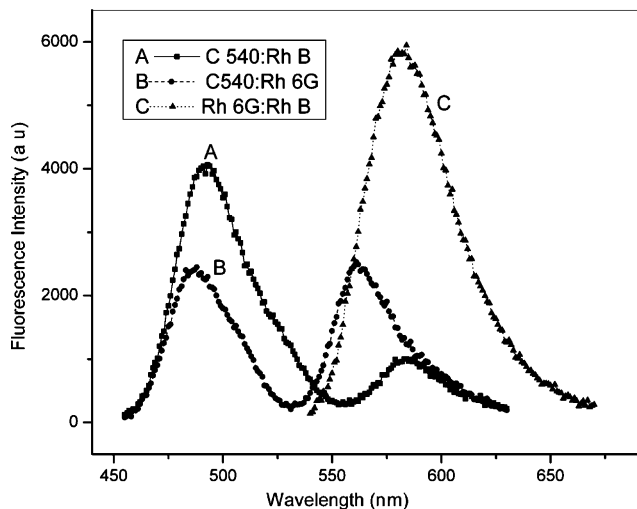


Fig. 4. Emission spectra of the dye mixtures in PMMA matrix. (A) $[D] = 10^{-5} \text{ mol l}^{-1}$ and $[A] = 7 \times 10^{-5} \text{ mol l}^{-1}$, (B) $[D] = 10^{-5} \text{ mol l}^{-1}$ and $[A] = 5 \times 10^{-4} \text{ m/l}$, (C) $[D] = 10^{-4} \text{ m/l}$ and $[A] = 5 \times 10^{-5} \text{ m/l}$.

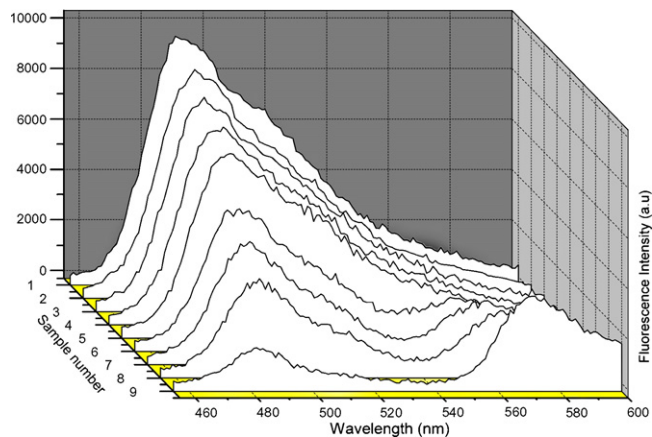


Fig. 5. The recorded fluorescence for the pair C 540:Rh 6G in MMA. Sample (1) $[D]$ only, (2) $[A] = 7 \times 10^{-6} \text{ m/l}$, (3) $[A] = 10^{-5} \text{ m/l}$, (4) $[A] = 10^{-5} \text{ m/l}$, (5) $[A] = 2.5 \times 10^{-5} \text{ m/l}$, (6) $[A] = 4 \times 10^{-5} \text{ m/l}$, (7) $[A] = 5.5 \times 10^{-5} \text{ m/l}$, (8) $[A] = 7 \times 10^{-5} \text{ m/l}$ and (9) $[A] = 10^{-4} \text{ m/l}$.

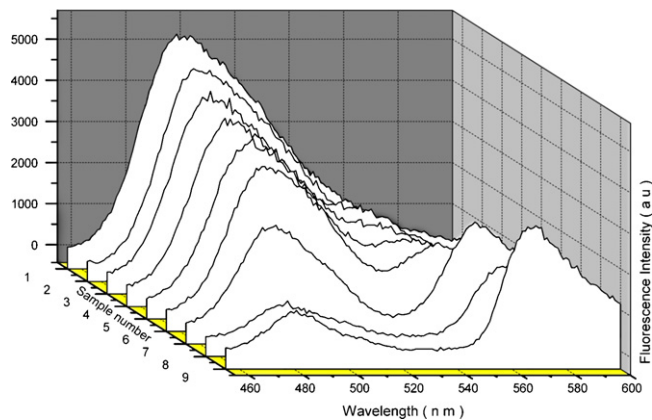


Fig. 6. The recorded fluorescence for the pair C 540:Rh 6G in PMMA. Sample (1) $[D]$ only, (2) $[A] = 7 \times 10^{-6} \text{ m/l}$, (3) $[A] = 10^{-5} \text{ m/l}$, (4) $[A] = 10^{-5} \text{ m/l}$, (5) $[A] = 2.5 \times 10^{-5} \text{ m/l}$, (6) $[A] = 4 \times 10^{-5} \text{ m/l}$, (7) $[A] = 5.5 \times 10^{-5} \text{ m/l}$, (8) $[A] = 7 \times 10^{-5} \text{ m/l}$ and (9) $[A] = 10^{-4} \text{ m/l}$.

different in the two matrices. The concentrations are 7×10^{-5} , $5.5 \times 10^{-5} \text{ m/l}$, respectively, for MMA and PMMA matrices for the pair C 540:Rh 6G. A similar kind of variation was observed in C 540:Rh B pair as well.

5. Dependence of peak emission wavelengths on acceptor concentration

From the recorded fluorescence in Figs. 5 and 6 an important observation is that in the mixture, donor dye always shows a blue shift. In MMA matrix, for the C 540:Rh 6G pair, the donor blue shift was found to be 9 nm while for the C 540:Rh B pair the shift was about 7 nm. In the absence of donor, the acceptor emission showed a continuous red shift of about 9 nm in the range of concentrations from 10^{-5} to 10^{-4} m/l for the C 540:Rh 6G pair and this red shift was about 11 nm for the pair C 540:Rh B in the concentration range, 10^{-4} to $7 \times 10^{-4} \text{ m/l}$. But in the presence of donor, both the acceptors showed an initial blue shift followed by a red shift. For the dye pair C 540:Rh 6G, a distinct peak for the acceptor arises at an acceptor concentration

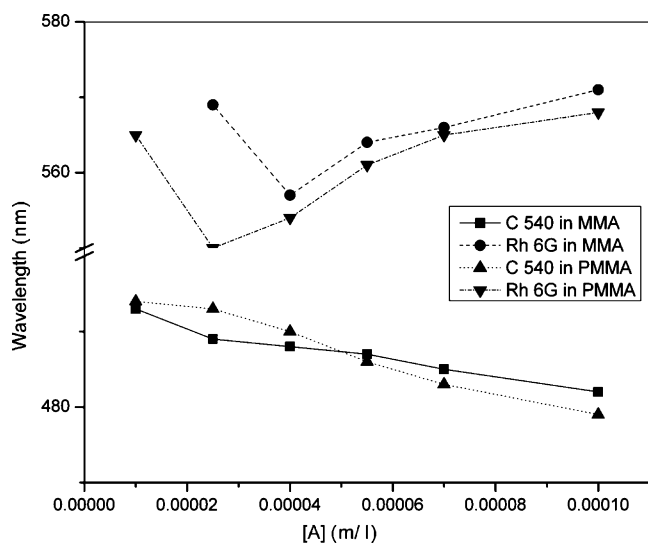


Fig. 7. The variation of donor and acceptor emission peak wavelength in the dye mixture C 540:Rh 6G with acceptor concentration.

4×10^{-5} m/l and this was blue shifted by 4 nm compared to the pure acceptor emission peak at that concentration. Above this acceptor concentration, acceptor emission peaks are red shifted by about 18 nm. A similar behaviour was observed for the C 540 Rh B pair also where distinct peak for the acceptor emission arises at $[A] = 5 \times 10^{-4}$ m/l with a blue shift of about 10 nm followed by a red shift of 12 nm up to $[A] = 7 \times 10^{-4}$ m/l. The above analysis was not made for the Rh 6G:Rh B pair since there was only a single peak in the emission spectrum. Fig. 7 shows the dependence of donor and acceptor wavelengths on acceptor concentration in MMA as well as PMMA matrices for the pair C 540:Rh 6G. The figure clearly shows that, the blue shifts of the donor emission as well as the red shift in the acceptor emission in the present range of acceptor concentrations are larger for the dye mixture in PMMA. In MMA, the initial blue shift for the acceptor was about 12 nm, which was followed by a red shift of about 14 nm while for the dye mixture in PMMA, the acceptor shows an initial blue shift of about 15 nm followed by a red shift of 18 nm. In PMMA, the donor dye shows a continuous blue shift of about 15 nm. The additional feature in dye mixture in PMMA is that, the acceptor peak becomes more distinct at a lower value of $[A]$.

The blue shift observed in the donor emission can be attributed to the fact that at smaller intermolecular separations, the heat energy generated in the acceptor system will be sufficient to populate the higher excited singlet state of the donor molecule. The sudden blue shift observed for the acceptor molecule is the result of the energy transfer process. The donor-sensitised system was observed to have a higher gain compared to an unsensitised system due to an increase in the effective lifetime [13]. As a result of this, the gain maximum is shifted towards the blue region. The lifetime of the acceptor will be appreciably increased at low concentrations ($<10^{-3}$ mol) as reported by Urisu and Kajiyama [25]. Similar blue shifts have been reported in Rh 6G:Rh B dye mixture in ethanol [26] and also in other dye mixtures [27,28]. During energy transfer process at

lower $[A]$ values, many acceptor molecules are excited to its higher excited singlet states and the consequent emission gives rise to this blue shift. At higher acceptor concentrations, this effect is not dominant because of the collisional de-excitation. A reduction in the non-radiative relaxation rate occurring in the excited state manifold could also be a reason for the blue shift observed here. Evidently the rate of such relaxation must be getting enhanced at higher concentrations. The red shift beyond a certain acceptor concentration is also attributed to the fact that with increase in concentration, both absorption and fluorescence intensities increase and a change in the reabsorption pattern occurs. For these concentrations, the acceptor emission depends only on its concentration and the energy transfer effect will not have any dependence on the emission wavelength of the acceptor molecule.

6. Dependence of peak fluorescence intensity of donor and acceptor on acceptor concentration

It is important to know the relative fluorescence intensities of the two peak emissions in the mixture before the solution is polymerised. In all the three pairs, considerable increase in fluorescence intensities were obtained at the acceptor emission wavelengths compared to the pure acceptor fluorescence. Specifically, in the pair C 540:Rh B, the acceptor dye Rh B starts emission from the $[A] = 7 \times 10^{-5}$ m/l onwards whereas in the entire concentration range of the present study, the pure acceptor does not have any significant emission. Fig. 8 shows the variation of the emission intensity of the donor and acceptor molecules with acceptor concentration for the present ETDL system. It was observed that, the fluorescence intensity of the acceptor was increased by 4.1 times in the range of acceptor concentrations in the present ETDL system with maximum intensity being at $[A] = 1 \times 10^{-4}$ m/l. But at very high acceptor concentrations ($>1 \times 10^{-4}$ m/l), curves show a decrease in slope, which is due to the self-quenching acceptor–acceptor interaction. At the

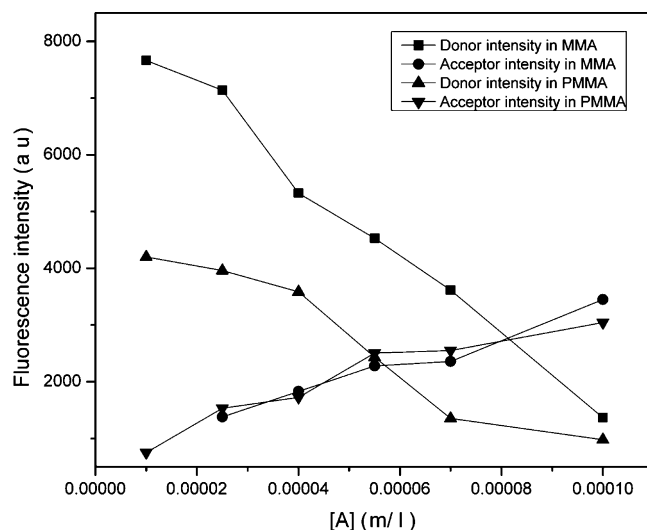


Fig. 8. The variation of donor and acceptor fluorescence with acceptor concentration for the C 540:Rh 6G pair.

same time, the donor emission intensity decreases considerably with increasing acceptor concentrations. It also clearly depicts the enhancement of the acceptor fluorescence in the range of concentrations of the present study compared to the pure acceptor. A similar enhancement in the acceptor emission was also observed in C 540:Rh B pair also. For the Rh 6G:Rh B pair, even though there were no distinct peaks for donor and acceptor, the intensity measurements at the donor and acceptor wavelengths showed almost a similar behaviour.

It may be pointed out that the pure acceptors Rh 6G and Rh B are not having any significant emission at 445 nm excitation even though there is a little fluorescence from the Rh 6G at higher acceptor concentrations ($\geq 10^{-4}$ m/l). In the presence of donor, the acceptor emission becomes more efficient due to effective energy transfer from the donor. Another important feature is that there is a comparable intensity for the acceptor both in MMA as well as PMMA matrices even though there is considerable reduction in the intensity for the donor after polymerisation.

This comparable intensity for acceptor in the two matrices as shown in Fig. 8 is attributed to the fact that polymerisation in the present experiment results in higher values of radiative and non-radiative energy transfer rate constants from donor to acceptor which in turn compensates the possible decrease in acceptor intensity after polymerisation.

7. Energy transfer rate constants

In the presence of acceptor dye, the fluorescence intensity of the donor dye is reduced from I_{0d} to I_d . The energy transfer efficiency and the transfer rate constants for the ETDL system in MMA and PMMA matrices can be calculated by studying the relative fluorescence intensities of the donor (I_{0d}/I_d). In MMA matrix, for the pair C 540:Rh 6G, the transfer efficiency assumes maximum values at the highest acceptor concentration. It starts from a minimum value (~ 0.26) at the lowest acceptor concentration 10^{-5} m/l to a maximum value (~ 0.63) at the highest concentration 10^{-4} m/l. For the pair C 540:Rh B, the transfer efficiency varies from (~ 0.23) at $[A] = 10^{-4}$ m/l to (~ 0.56) at 7×10^{-4} m/l. In the case of Rh 6G:Rh B pair, the transfer efficiency was 0.25 at $[A] = 3.5 \times 10^{-5}$ m/l to 0.8 at $[A] = 10^{-4}$ m/l. The maximum values of efficiencies in the PMMA matrix were 0.76, 0.64 and 0.87 for C 540:Rh 6G, C 540:Rh B and Rh 6G:Rh B pairs, respectively. Knowing the value of $[A]_{1/2}$ the half quenching concentration at which $I_d = I_{0d}/2$, the value of critical radius R_0 can be evaluated using Eq. (3) for the three dye pairs.

After polymerisation, all the samples show a faster quenching compared to the dye mixtures in monomer. Fig. 9 shows the Stern–Volmer plots obtained for the dye mixtures both in MMA as well as PMMA. There is a clear indication of the change in slope after the medium is solidified which essentially leads to changes in the energy transfer characteristics of the system.

The values obtained for R_0 clearly shows that the non-radiative transfer involved in the dye mixture is of dipole-dipole in nature. There are noticeable changes in the R_0 values in

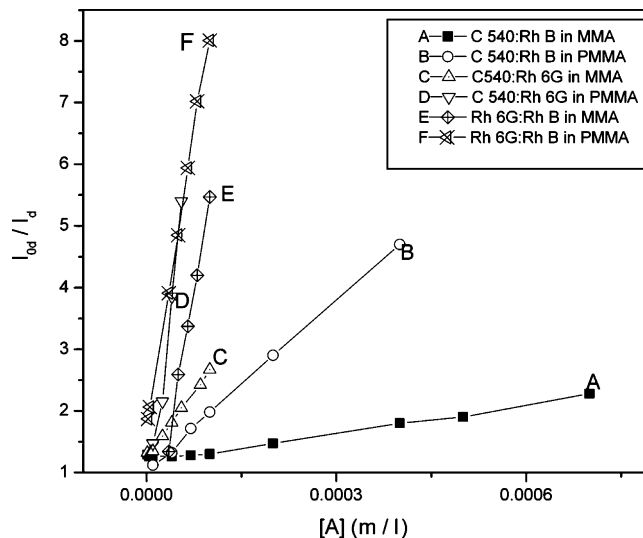


Fig. 9. The Stern–Volmer plots for the present ETDL systems.

PMMA as compared with the values in MMA. For C 540:Rh 6G pair, R_0 changed from 195 to 242 Å. The changes in the other dye pairs were 91–156 and 210–340 Å for C 540:Rh B and Rh 6G:Rh B pairs, respectively. The fluorescence lifetimes of the pure donor molecules in MMA as well as PMMA were measured experimentally using time-correlated single photon counting technique. Figs. 10 and 11 show fluorescence decay curves of the pure donor molecules in MMA. The measured values of the lifetimes were $\tau_{0d} = 4.96$ and 8.00 ns for C 540 and Rh 6G, respectively. Figs. 12 and 13 depict the decay curves for donor molecules in the PMMA giving the lifetime values as 4.99 and 9.95 ns for C 540 and Rh 6G, respectively. Using these values of τ_{0d} , the total energy transfer rate constants (K_T) were calculated from the slopes of the Stern–Volmer plots.

The non-radiative transfer efficiencies were evaluated using Eq. (6) for different $[A]$ values and hence a comparison between

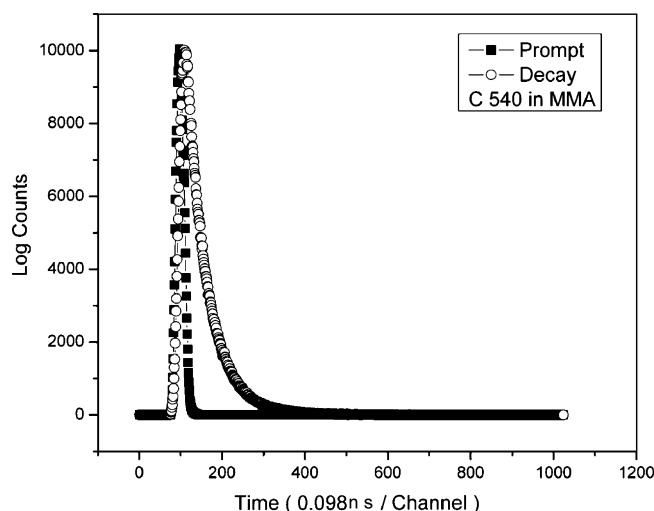


Fig. 10. The fluorescence decay curve of the donor C 540 in MMA.

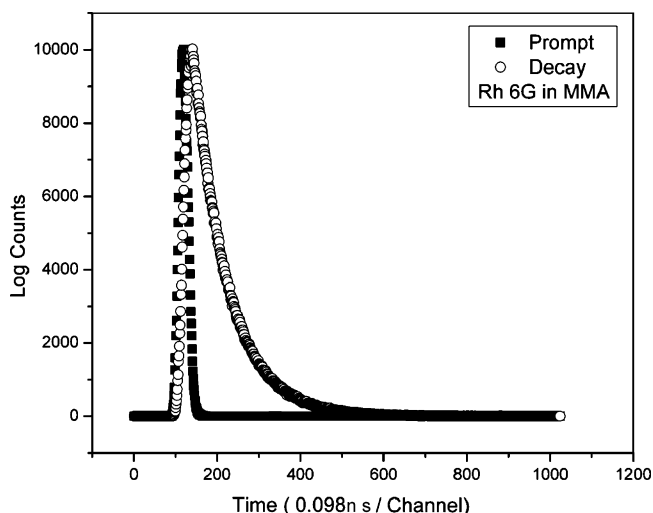


Fig. 11. The fluorescence decay curve of the donor Rh 6G in MMA.

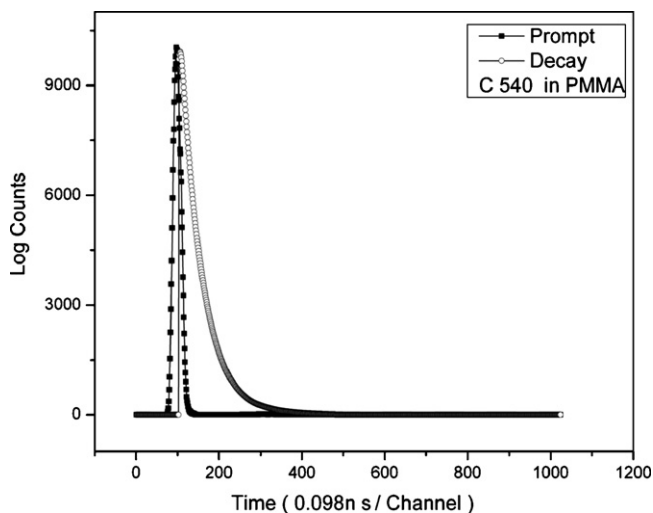


Fig. 12. The fluorescence decay curve of the donor C 540 in PMMA.

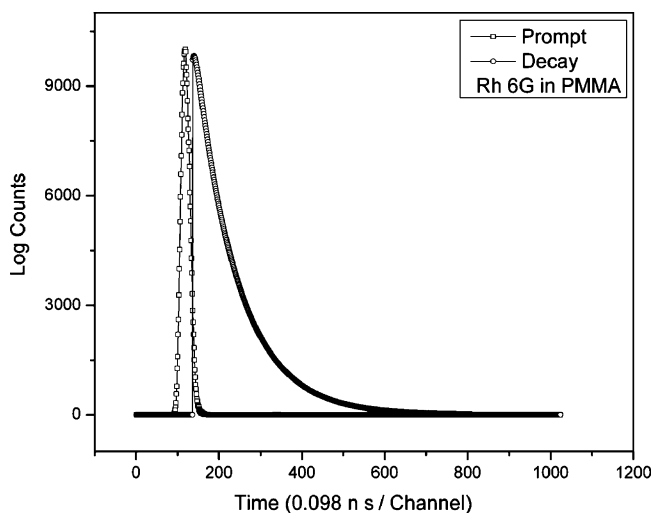
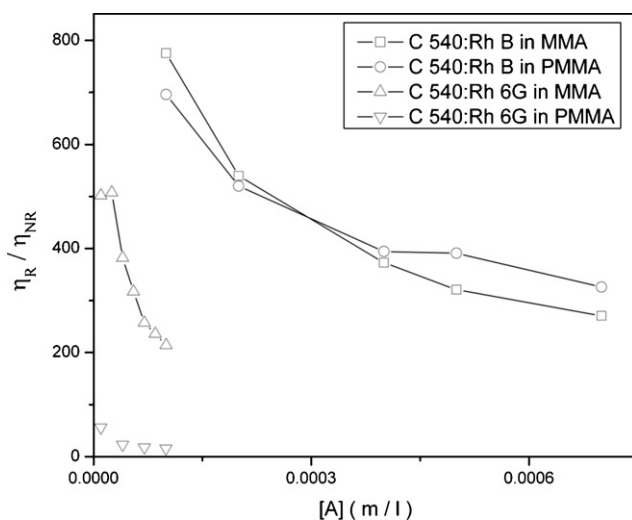
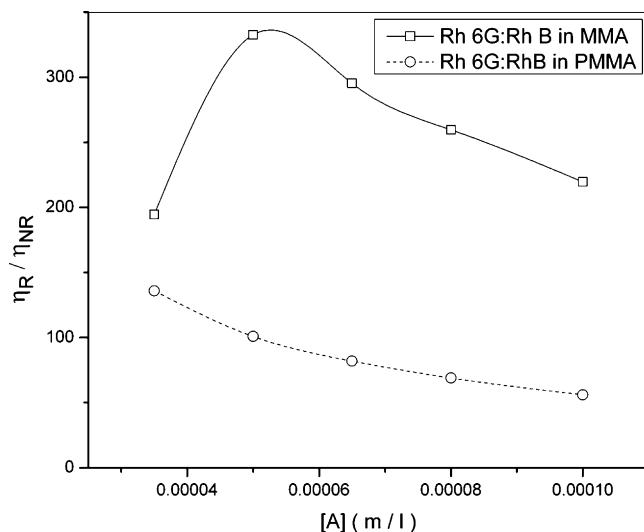


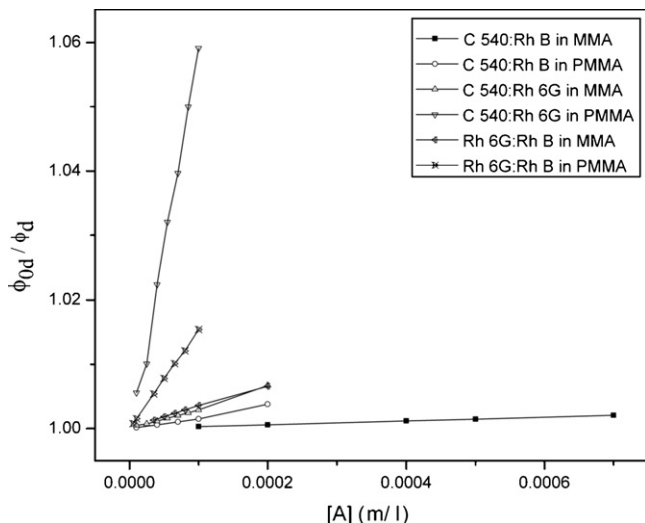
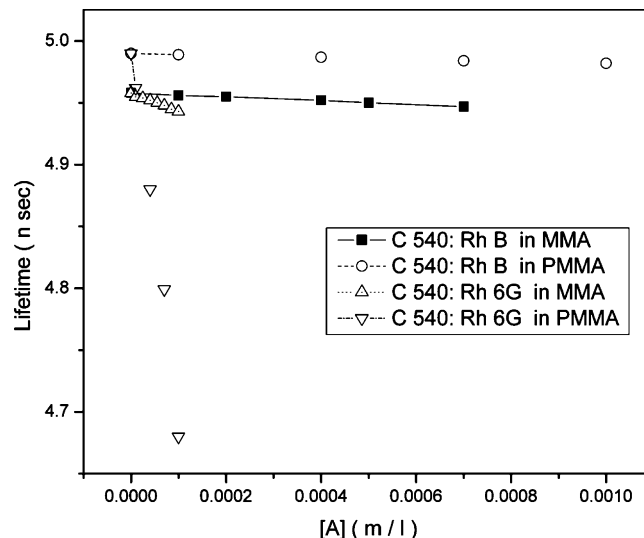
Fig. 13. The fluorescence decay curve of the donor Rh 6G in PMMA.

Fig. 14. Plot of η_r/η_{nr} vs. $[A]$ for C 540:Rh B pairs in MMA and PMMA.

the radiative and non-radiative contributions to the energy transfer mechanism can be made by plotting a graph between η_r/η_{nr} and $[A]$. Figs. 14 and 15 show such graphs and the minimum value of the ratio η_r/η_{nr} was found to be ~ 14 for the dye pair, C 540:Rh 6G in PMMA.

The present study gives us a clear idea about the relative magnitudes of the energy transfer mechanisms occurring in the mixtures. The result clearly indicate that non-radiative transfer part is comparatively less important than the radiative transfer mechanism in the present ETDL systems even though the non-radiative part shows an increase in its values at higher acceptor concentrations. For the pair, C 540:Rh 6G in PMMA, it was observed that the non-radiative part is considerably increased compared to the mixture in MMA. This can be the reason for the fast quenching in this dye pair compared to the other two. In Fig. 15, for the dye mixture in MMA, the magnitude of η_r is very low so that η_r/η_{nr} is small at low acceptor concentrations.

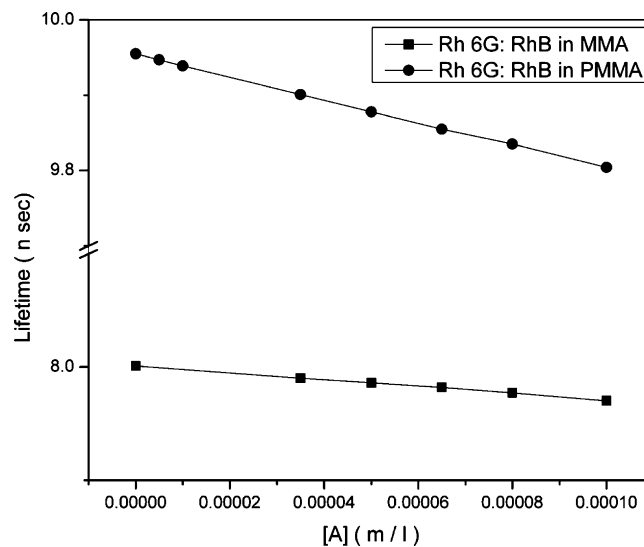
Fig. 15. Plot of η_r/η_{nr} vs. $[A]$ for Rh 6G:Rh B pair.

Fig. 16. Plot of ϕ_{0d}/ϕ_d vs. $[A]$ for the three dye pairs in MMA and PMMA.Fig. 17. Plot of τ_d vs. $[A]$ for the C 540:Rh 6G and C 540:Rh B pairs.

The ratio reaches a maximum at an acceptor concentration of 5×10^{-5} m/l beyond which η_{nr} enhances rapidly which is clear as seen in the figure.

By knowing the value of η_{nr} at different acceptor concentrations, the relative quantum yields of the donor molecules (ϕ_{0d}/ϕ_d) in MMA as well as PMMA were calculated. The values of non-radiative transfer rate K_{nr} can be directly evaluated from the slope of the graph between ϕ_{0d}/ϕ_d and $[A]$ (Fig. 16) which is also a straight line obeying the Stern–Volmer expression.

Also by knowing the values of τ_{0d} and ϕ_{0d}/ϕ_d , the value of τ_d , the fluorescence lifetime of the donor in the presence of acceptor at various acceptor concentrations can be evaluated. Figs. 17 and 18 show the variation in the lifetimes of the donor molecules in the presence of acceptors. It is clear that the fluorescence lifetime of the donor molecules are not affected much due to the energy transfer mechanism, which again confirms the dominance of radiative type of energy transfer except for the pair, C 540:Rh 6G in PMMA where there is a considerable non-radiative contribution. The kind of changes in the donor lifetime shows that there is noticeable increase in the non-radiative energy transfer mechanism in this system. Another observation is that, the pure donors showed an enhancement in the lifetime after the polymerisation. The changes

Fig. 18. Plot of τ_d vs. $[A]$ for the Rh 6G:Rh B pair.

were from 4.96 and 8.00 to 4.99 and 9.95 ns, respectively, for the C 540 and Rh 6G, respectively. The calculated values of τ_d in MMA as well as PMMA for the pair C 540:Rh 6G at $[A] = 4 \times 10^{-5}$ m/l were about 4.95 and 4.88 ns, respec-

Table 1
Calculated parameters for the energy transfer

Parameter	C 540:Rh B ^a	C 540:Rh B ^a	C 540:Rh 6G ^a	C 540:Rh 6G ^a	Rh 6G:Rh B ^a	Rh 6G:Rh B ^a
	MMA ^b	PMMA ^b	MMA ^b	PMMA ^b	MMA ^b	PMMA ^b
K_r ($\times 10^9$ s ⁻¹)	322	485	2836	8893	7699	6824
K_{nr} ($\times 10^9$ s ⁻¹)	0.59	0.67	5.53	118	4.37	15.4
R_0 (A ⁰)	90.7	94.5	195	242	210	340
$[A]_{1/2}$ (M)	5.38×10^{-4}	4.7×10^{-4}	5.3×10^{-5}	2.8×10^{-5}	4.3×10^{-5}	1.01×10^{-5}
τ_{0d} ($\times 10^9$ s ⁻¹)	4.96	4.99	4.96	4.99	8.00	9.96
τ_d ($\times 10^9$ s ⁻¹) (at $[A] = 7 \times 10^{-4}$ M)	4.94	4.97	4.95 (at $[A] = 7 \times 10^{-5}$ M)	4.79	7.97 (at $[A] = 7 \times 10^{-4}$ M)	9.86

^a Dye pair.

^b Matrix.

tively. These values of τ_d were also measured experimentally using the transient single photon counting technique and was found to be 4.96 and 4.84 ns. Table 1 summarises the various calculated parameters of the dye mixture in MMA and PMMA.

8. Conclusions

A series of dye mixture doped polymer rods were fabricated which simultaneously emit two wavelengths at different relative intensities. The shifts in these wavelengths with acceptor concentration provides a wide range tunability. We have analysed in detail the energy transfer process in the dye pairs C 540:Rh 6G, C 540:Rh B and Rh 6G:Rh B in methyl methacrylate and poly(methyl methacrylate). The lifetimes of the pure donor and the dye mixture in MMA and PMMA were experimentally determined. Enhancements of lifetimes were observed for the pure donor dyes in PMMA matrix. It was observed that, the fluorescence intensity of the acceptor dyes were increased many times within the range of acceptor concentrations studied. Acceptor concentration dependence of the energy transfer, the blue shift in the donor molecules and the variations in the donor lifetime clearly show that the radiative energy transfer process is having a major contribution in the present ETDL system. By suppressing the undesirable triplet state formation, the immobilisation of the dye molecules in PMMA leads to overall enhancement in the efficiency of the system. We recognize that our results could forecast suitable concentration regions for the wavelength shifts and intensity variations with the acceptor concentration for the dye mixture. The shifts in the wavelengths of both donors as well as acceptors were also studied which will enable us to choose from a variety of polymer rods to fabricate solid-state dye lasers and polymer optical fibre amplifiers operating in multi-wavelength regime.

References

- [1] D.J. Taylor, S.E. Harris, S.T.K. Nieh, T.W. Hansch, *Appl. Phys. Lett.* 19 (269) (1971).
- [2] E.F. Salewski, R.A. Keller, *Appl. Opt.* 10 (1971) 2773.
- [3] H.S. Pilloff, *Appl. Phys. Lett.* 21 (1972) 339.
- [4] C.Y. Wu, J.R. Lombardi, *Opt. Commun.* 7 (1973) 233.
- [5] O.G. Peterson, B.B. Snavelly, *Bull. Am. Phys. Soc.* 13 (1968) 397.
- [6] S.A. Ahmed, J.S. Gergerly, *J. Chem. Phys.* 61 (1974) 1584.
- [7] Y. Yap, T. Tou, K. Kwek, *Jpn. J. Appl. Phys.* 35 (1996).
- [8] P. Burlsmacchi, H.F.R. Sandoval, *Opt. Commun.* 31 (1979) 185.
- [9] Y. Saito, N. Nakai, A. Nomura, T. Kano, *Appl. Opt.* 31 (1992) 4298–4304.
- [10] C.E. Moller, C.M. Verber, A.H. Adelman, *Appl. Phys. Lett.* 13 (1971) 278.
- [11] A. Dienes, M. Madden, *J. Appl. Phys.* 44 (1973) 4161.
- [12] C. Lin, A. Dienes, *J. Appl. Phys.* 44 (1973) 5050.
- [13] T. Urisu, K. Kajiyama, *J. Appl. Phys.* 47 (1976) 3563.
- [14] D.A. Gramov, K.M. Dyumaev, A.A. Manenkov, A.P. Maslyakov, *J. Opt. Soc. Am. B* 2 (1985) 1028.
- [15] R.E. Hermes, *SPIE* 2116 (1994) 178.
- [16] M. Rajesh, K. Geetha, C.P.G. Vallabhan, P. Radhakrishnan, V.P.N. Nampoore, *Appl. Opt.* 46 (1) (2007) 106.
- [17] A. Tayaga, S. Teramoto, T. Yamamoto, K. Fujii, E. Nihei, Y. Koike, K. Sasaki, *IEEE J. Quantum Electron.* 31 (12) (1995) 2215.
- [18] G.D. Peng, Z. Xiong, Peng, P.L. Chu, *J. Lightwave Technol.* 16 (12) (1998) 2365.
- [19] M.A. Ali, S.A. Ahmed, *J. Chem. Phys.* 90 (1989) 1484.
- [20] D. Mohan, S. Sanghi, R.D. Singh, *J. Photochem. Photobiol. A: Chem.* 68 (1992) 77.
- [21] R.D. Singh, A.K. Sharma, N.V. Unnikrishnan, D. Mohan, *Pramana-J. Phys.* 34 (1990) 77.
- [22] M.A. Ali, S.A. Ahmed, *Appl. Opt.* 29 (1990) 4494.
- [23] J.B. Birks, M.S.S.C.P. Leite, *J. Phys. B* 3 (1970) 513.
- [24] T. Govindanunny, B.M. Sivaram, *J. Lumin.* 21 (1980) 397.
- [25] T. Urisu, K. Kajiyama, *J. Appl. Phys.* 47 (1976) 3559.
- [26] P.J. Sebastian, K. Sathyanandan, *Opt. Commun.* 35 (1980) 113.
- [27] G.A. Kumar, N.V. Unnikrishnan, *J. Photochem. Photobiol. A* 144 (2001) 107.
- [28] M. Kailasnath, G.A. Kumar, V.P.N. Nampoore, *Proceedings of Photonics 2004 7th International Conference on Optoelectronics Fibre Optics and Photonics, Kochi, India, 9–11 December, 2004*, p. 400.